

Spatial Routing at 125 Gbit/s Based on Noncollinear Generation of Self-trapped Beams in Ti:PPLN Film Waveguides

Paul-Henri Pioger, Fabio Baronio, Vincent Couderc, Alain Barthélémy, *Member, IEEE*, Costantino De Angelis, Yoohong Min, Victor Quiring, and Wolfgang Sohler, *Associate Member, IEEE*

Abstract—We investigated numerically and experimentally spatial switching and spatial steering of optical beams based on the noncollinear excitation of self-trapped waves in a quadratic nonlinear medium. The two input fields at the fundamental frequency give birth either to a single spatial soliton or to two separate solitons. Their propagation directions and their location on the output face of the crystal are conditioned by the phase difference between the input beams. An all-optical ultra fast switch based on that scheme was then implemented in a periodically poled lithium niobate film waveguide. Pulse dropping in a 125 Gbit/s pulse train at 1548 nm has been demonstrated.

Index Terms—Film PPLN waveguide, group velocity mismatch, self trapping, spatial switching.

I. INTRODUCTION

SINCE the 1970s, self guided optical beams, in particular quadratic spatial solitons (QSSs), are numerically and experimentally studied for their potential application to all optical switching and routing [1], [2]. QSSs consist of multifrequency waves strongly coupled by second order nonlinearity $\chi^{(2)}$; QSSs result from the mutual trapping and locking of the different frequency components through parametric interactions. These types of solitary waves are stable and robust in guided and in bulk geometries. Numerical and experimental investigations have already demonstrated the possibilities offered by QSSs to realize all optical addressing devices by soliton collision in one and two dimensions. Repulsion, fusion, spiraling, and spatial steering of QSSs were already demonstrated and studied [3]–[8].

In this paper, we refer to nonlinear type I interaction of a fundamental wave [(FF) at 1548 nm] and a second-harmonic wave [(SH) at 774 nm]. We investigated, for the first time to our knowledge, spatial interactions of two optical beams, launched simultaneously along different directions and superimposed on

Manuscript received July 25, 2003; revised September 5, 2003. This work was performed in the frame of the European project ROSA (IST/FET), supported by the European Commission.

P.-H. Pioger, V. Couderc and A. Barthélémy are with the Faculté des Sciences, I.R.C.O.M., 87060 Limoges, France (e-mail: coudercv@ircm.unilim.fr).

F. Baronio is with Istituto Nazionale per la Fisica della Materia, Università di Padova, 35131 Padova, Italy.

C. De Angelis is with Istituto Nazionale per la Fisica della Materia, Università di Brescia, 25123 Brescia, Italy.

Y. Min, V. Quiring and W. Sohler are with Universität Paderborn, 33095 Paderborn, Germany.

Digital Object Identifier 10.1109/LPT.2003.822264

the input face of a periodically poled Ti-indiffused lithium niobate (Ti:PPLN) slab waveguide. The number and the location of the generated quadratic quasi-solitons are controlled by the phase relationship between the FF input beams. The experiments were performed using picosecond pulses shorter than the group time delay (GTD) between the FF and the SH during their propagation in the PPLN and with only the FF beams at the input. Experimental results are in good qualitative agreement with the numerical simulations. Finally, we experimentally demonstrated an all optical spatial switching with high efficiency at a repetition rate of 125 Gbit/s.

II. EXPERIMENTAL SETUP

The experiments were performed with a 63 mm long and 10 mm width planar waveguide fabricated in a z-cut LiNbO₃ substrate by indiffusion of a 70 nm thick, vacuum-deposited Ti-layer at 1060 °C. An uniform microdomain structure of $\Lambda = 16.4 \mu\text{m}$ periodicity (duty cycle 0.5) has been generated after waveguide fabrication by electric field assisted poling. The sample is inserted in a temperature stabilized oven to allow operation at elevated temperatures ($T = 120\text{--}290^\circ\text{C}$); temperature-tuning of the phase-matching conditions becomes possible.

An all-fiber laser system is used as the source of 4 ps pulses (full width at half maximum FWHM) at 1548 nm (FF) and of a peak power of a few kW at 20 MHz repetition rate. The spectral bandwidth of the input beam is 1.7 nm, which represents 5.3 times the spectral acceptance bandwidth of the PPLN. The thickness of the waveguide permitted the propagation of a single TM₀ mode of 4 μm width at the FF; several TM modes are supported at the SH, but only the TM₀ of 3 μm width is efficiently pumped by the TM₀ at the FF.

A Michelson-type Interferometer (MI) splits the beam at the FF into two separate waves of equal energy. The two beams are then superimposed on the input face of the nonlinear medium, with a crossing angle of 0.4°. Each beam is shaped in a highly elliptical spot, nearly gaussian in profile, with $w_{ox} = 60 \mu\text{m}$ (FWHM) along the waveguide plane and $w_{oz} = 3.9 \mu\text{m}$ along the perpendicular direction and is polarized parallel to the z axis of the PPLN for access to the material's largest quadratic non-linear coefficient $\chi_{zzz}^{(2)} = 54 \text{ pm/V}(2d_{33})$. The spatial beam profiles are recorded by scanning a magnified image of the pattern with a photodiode. Temporal characterizations are monitored by a noncollinear SH-generation autocorrelator.

III. NUMERICAL MODEL

We model the electric fields E_1 and E_2 , at ω_0 (FF) and $2\omega_0$ (SH) respectively, with $\omega_0 = 2\pi c/\lambda_0$ and $\lambda_0 = 1548$ nm free space wavelength, propagating in the y direction, as

$$\begin{aligned} E_1(x, y, z, t) &= \frac{1}{2} \left[m_1(z) a_1(x, y, t) \right. \\ &\quad \times \exp(-j(\beta_{\omega_0} y + \omega_0 t)) + cc \left. \right] \\ E_2(x, y, z, t) &= \frac{1}{2} \left[m_2(z) a_2(x, y, t) \right. \\ &\quad \times \exp(-(\beta_{2\omega_0} y + 2\omega_0 t)) + cc \left. \right] \quad (1) \end{aligned}$$

where $m_1(z)$ and $m_2(z)$ are the mode profiles in the guided dimension, and $a_1(x, y, t)$ and $a_2(x, y, t)$ are the slowly varying envelopes. The envelopes $a_1(x, y, t)$ and $a_2(x, y, t)$ obey the nonlinear coupled equations [9]:

$$\begin{aligned} j \frac{\partial a_1}{\partial y} - j \beta'_{\omega_0} \frac{\partial a_1}{\partial t} - \frac{\beta''_{\omega_0}}{2} \frac{\partial^2 a_1}{\partial t^2} + \frac{1}{2\beta_{\omega_0}} \frac{\partial^2 a_1}{\partial x^2} \\ + \frac{\chi^{(2)} \omega_0}{2c n_{\omega_0}} \frac{\int m_2 |m_1|^2 dz}{\int |m_1|^2 dz} a_2 a_1^* e^{-j\Delta ky} = 0 \\ j \frac{\partial a_2}{\partial y} - j \beta'_{2\omega_0} \frac{\partial a_2}{\partial t} - \frac{\beta''_{2\omega_0}}{2} \frac{\partial^2 a_2}{\partial t^2} + \frac{1}{2\beta_{2\omega_0}} \frac{\partial^2 a_2}{\partial x^2} \\ + \frac{\chi^{(2)} \omega_0}{2c n_{2\omega_0}} \frac{\int m_2 |m_1|^2 dz}{\int |m_2|^2 dz} a_1^2 e^{j\Delta ky} = 0 \quad (2) \end{aligned}$$

where β represents the propagation constant, β' the inverse group velocity, β'' the inverse group-velocity dispersion; n is the refractive index, $\Delta k = 2\beta_{\omega_0} - \beta_{2\omega_0} + K_S$, where $K_S = 2\pi/\Lambda$ and $\chi^{(2)} = (2/\pi)\chi_{zzz}^{(2)}$ is the nonlinear coefficient. To model the pulse propagation, two different numerical tools are used. We employ a finite-difference vectorial mode solver to determine the linear propagation properties in the slab waveguide, i.e., the mode profiles, β_{ω_0} , $\beta_{2\omega_0}$, β'_{ω_0} , $\beta'_{2\omega_0}$, β''_{ω_0} and $\beta''_{2\omega_0}$. The crystal length L corresponded to 5.6 times to the diffraction length (Rayleigh range) associated to the FF input beams and to 5.2 times the group velocity mismatch length between FF and SH; the dispersive terms can be neglected. Finally, using a finite-difference beam propagation technique, we solved the nonlinear coupled equations (2).

IV. INVESTIGATIONS

Experiments and numerical simulations are realized by launching simultaneously two FF input beams in the film waveguide, with two different directions. The two beams are superimposed on the input face of the nonlinear medium, with a crossing angle of 0.4° . The phase relationship between the beams is controlled by the modification of one arm of the interferometer. The investigations are carried on under conditions for which each FF input beam alone can give birth to a QSS.

It was demonstrated that because of the presence of a large group velocity mismatch, spatial soliton propagation of few picosecond pulses is obtained only at positive phase-mismatch, above an intensity threshold [10]. In our experimental conditions, spatial trapping of a single FF beam starts to appear at a sample temperature of 270°C ($\Delta k L \sim 9\pi$), at intensity

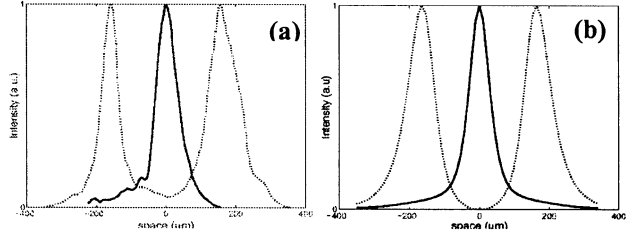


Fig. 1. (a) Measured and (b) calculated spatial beam profiles of the FF output for a zero (solid curves) and π (dotted curves) phase difference between the FF input waves. The two FF input beams are superimposed on the input face of the nonlinear medium, with a crossing angle of 0.4° . Here $I = 85$ MW/cm 2 , $\Delta k L = 9\pi$ for both cases (a) and (b).

threshold $I = 85$ MW/cm 2 and is maintained (with a linear increase of the intensity threshold) down to $T = 180^\circ\text{C}$ ($\Delta k L \sim 100\pi$), at intensity threshold $I = 600$ MW/cm 2 .

In our case, the number and the direction of propagation of the generated solitary waves are determined by the spatial distribution of the input power close to the input face of the crystal. For a zero phase difference between the input FF waves, the interferences between the two waves leads to a single central lobe and a single quadratic solitary wave is excited by fusion of the two input beams. The propagation direction of the excited soliton corresponds to the median direction between the two input beams directions [Fig. 1 (solid curve)]. Moreover, a continuous change of the phase relationship between the input waves allows to realize a slight steering of the output position of the single trapped beam. For a π phase difference between the FF input beams, the interaction between the beams on the input face of the PPLN leads to spatial fringes with two main lobes. So, two separated solitary waves are excited with their propagation directions parallel with the input direction of each beam [Fig. 1 (dotted curves)]. The behaviors derived from numerical simulations are in good agreement with the behaviors obtained in experiments and confirmed the phase dependence of the output patterns.

The superimposition of the two FF input beams on the input face of the crystal is not critical. It is important that the spatial interaction of the beams takes place before the formation of two well defined quadratic quasi-solitons. Spatial switching and steering operate while the self trapping regime of the input beams is not completely reached. Beyond this limit, the behavior of the interactions changes; we can speak of quasi-soliton collisions. In this case, because spatial soliton propagation is obtained only at large positive phase-mismatch, they resemble Kerr soliton crossing, passing through each other (elastic collision) for any initial phase differences [6].

Finally, we demonstrated experimentally spatial switching of short pulses at high bit rates, based on soliton excitation and using a zero phase difference between the FF input waves. The aim is to spatially switch a single pulse (selected signal) among a high bit rate train of pulses using another noncollinear pulse (control). For a good temporal synchronization between the selected signal and control wave, the beams fuse, a single soliton is excited and propagates along the median direction; while the other pulses of the train propagate without perturbation along their original trajectories. A scheme of the experiment using the noncollinear spatial routing in the PPLN is displayed in Fig. 2.

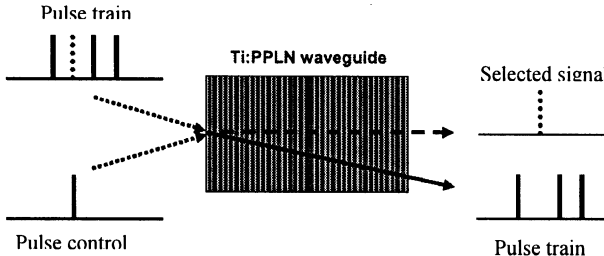


Fig. 2. Schematic representation of the spatial addressing mechanism.

To realize this experiment we used the previous set-up composed of a fiber laser source and a MI. The train of pulses (signal) is composed of a packet of pulses at a repetition rate of 20 MHz fixed by the laser. Each packet is composed by pulses of 4 ps duration (FWHM) separated by an adjustable delay. The data rate in the packet can be varied from 40 Gbit/s to 125 Gbit/s. This train is realized by a couple of parallel mirrors (one mirror is the rear mirror of one of the MI's arms, the other one is an extra partially reflecting mirror, $R = 50\%$) placed on one arm of the interferometer. The control beam is composed of a single pulse of 4 ps at a repetition rate of 20 MHz. The synchronization of the train of pulses with the control pulse is adjusted by changing the length of one arm of the interferometer. The two beams are further focused and superimposed with a weak tilt angle (0.4°) on the input face of the nonlinear waveguide. For a well temporal superposition of the signal and the control pulses, the two beams fuse. The single soliton propagates along the median direction with respect to their input directions. The signal pulse temporally selected by the control pulse is switched. The other pulses of the train propagate without perturbation along their initial trajectories. For a bit rate of 125 Gbit/s the autocorrelation trace of the output train shows clearly the spatial routing with a high efficiency. In this situation, the contrast (C) in the switched output is larger than 18 dB (at 125 Gbit/s) by reference to the satellite switched pulses. The input selected signal is depleted by 9–10 dB on the direct (nonswitched) output. Typical experimental autocorrelation traces and deduced temporal profiles of the FF input and output signals, at a data rate of 125 Gbit/s, relative to the switching of the second pulse of the train, are shown in Fig. 3.

V. CONCLUSION

In conclusion, we showed numerically and experimentally spatial switching and spatial steering of noncollinear optical beams based on a quadratic solitons excitation. The spatial interaction outcome, number and location of the excited solitons, is conditioned by the phase difference between the input beams.

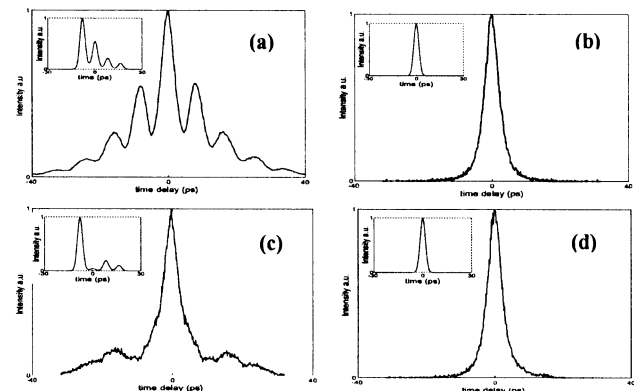


Fig. 3. Experimental autocorrelation trace and (inset) deduced temporal profile of the FF signals: (a) pulse train and (b) control pulse at the input. (c) Pulse train and (d) selected signal at the output.

These operations are carried out in a PPLN waveguide at 1548 nm. We also demonstrated experimentally spatial switching of short pulses at a repetition rate of 125 Gbit/s, based on solitons excitation with two in phase noncollinear beams.

REFERENCES

- [1] Y. N. Karamzin and A. P. Sukhorukov, "Nonlinear interaction of diffracting beams of light in a medium of quadratic nonlinearity, mutual focusing of beams and restriction of optical frequency convertor efficiency," *JETP Lett.*, vol. 20, pp. 339–342, 1974.
- [2] W. E. Torruellas, Z. Wang, D. J. Hagan, E. W. Vanstryland, G. I. Stegeman, L. Torner, and C. R. Menyuk, "Observation of two-dimensional spatial solitary waves in a quadratic medium," *Phys. Rev. Lett.*, vol. 74, pp. 5036–5039, 1995.
- [3] W. E. Torruellas, G. Assanto, B. L. Lawrence, R. A. Fuerst, and G. I. Stegeman, "All-optical switching by spatial walk-off compensation and solitary-wave locking," *Appl. Phys. Lett.*, vol. 68, pp. 1449–1451, 1996.
- [4] G. Leo and G. Assanto, "Collisional interactions of vectorial spatial solitary waves in type II frequency-doubling media," *J. Opt. Soc. Amer. B*, vol. 14, pp. 3151–3161, 1997.
- [5] V. Steblina, Y. S. Kivshar, and A. V. Buryak, "Scattering and spiraling of solitons in a bulk quadratic medium," *Opt. Lett.*, vol. 23, pp. 156–158, 1998.
- [6] R. Schiek, Y. Baek, G. I. Stegeman, and W. Sohler, "Interactions between one-dimensional quadratic soliton-like beams," *J. Opt. Quantum Electron.*, vol. 30, pp. 861–879, 1998.
- [7] A. Buryak, P. Di Trapani, D. Skryabin, and S. Trillo, "Optical solitons due to quadratic nonlinearities: from basic physics to futuristic applications," *Phys. Rep.*, vol. 370, pp. 63–235, 2002.
- [8] A. V. Buryak and V. V. Steblina, "Soliton collisions in bulk quadratic media: comprehensive analytical and numerical study," *J. Opt. Soc. Amer. B*, vol. 16, pp. 245–255, 1999.
- [9] G. I. Stegeman, D. J. Hagan, and L. Torner, " $\chi^{(2)}$ cascading phenomena and their applications to all optical signal processing, mode locking, pulse compression and solitons," *J. Opt. Quantum Electron.*, vol. 28, pp. 1691–1740, 1996.
- [10] P. Pioger, V. Couderc, L. Lefort, A. Barthelemy, F. Baronio, C. De Angelis, Y. Min, V. Quiring, and W. Sohler, "Spatial trapping of short pulses in ti-indiffused LiNbO₃ waveguides," *Opt. Lett.*, vol. 27, pp. 2182–2184, 2002.